INFN/AE-96/19
8 Luglio 1996

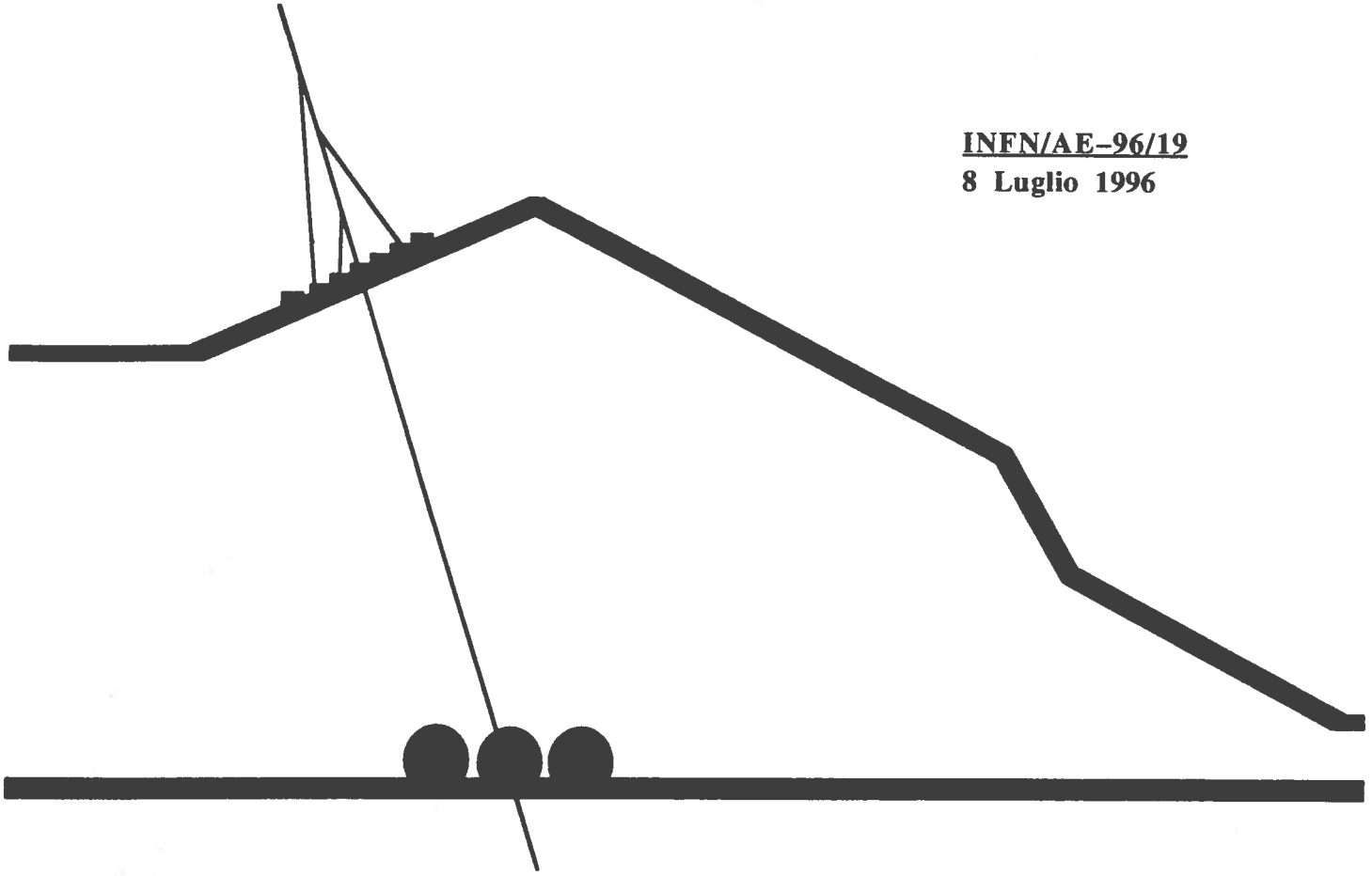

PHYSICS AND ASTROPHYSICS WITH MUTIPLE MUONS

G. Battistoni, O. Palamara

INFN - Laboratori Nazionali del Gran Sasso

Published by **SIS-Pubblicazioni**
dei Laboratori Nazionali di Frascati

INFN – Istituto Nazionale di Fisica Nucelare
Laboratori Nazionali del Gran Sasso

INFN/AE–96/19
8 Luglio 1996

PHYSICS AND ASTROPHYSICS WITH MULTIPLE MUONS

O. Palamara[1)], G. Battistoni[2)]
[1)] INFN–Sezione di Lecce, Via Arnesano, I–73100 Lecce, Italy
E–Mail: palamara@le.infn.it
[2)] INFN–Sezione di Milano, Via Celoria 16, I–20133 Milano, Italy
E–Mail: battistoni@mi.infn.it

Abstract

Multiple muon events observed in underground detectors open many windows on the physical world. One of the most established efforts is the study of the cosmic ray spectrum and composition in the interesting "knee" region of the primary spectrum via underground muon multiplicity distributions. Powerful deep underground detectors can perform additional analyses, which address other interesting topics. In addition to their intrinsic interest, these analyses are also relevant for our knowledge of cosmic ray themselves, and these efforts continue to improve our understanding and modelling of the fundamental processes which govern the cosmic ray cascade development.

1. Introduction

From the study of multiple muon events in deep underground detectors, it is possible to extract informations about the primary cosmic rays.

The high energy underground muons are remnant of the air showers produced in the atmosphere by collision of high energy cosmic ray nuclei with air nuclei. Muons are nearly stable and have a small cross section for interactions, so they are very penetrating. Indeed, muons are traditionally called the "penetrating component" of cosmic rays. Yet, because they are charged, they are relatively easy to detect. Thus, muons give the dominant signal deep in the atmosphere and underground. Underground muons are produced in the highest energy part of the atmospheric cascades at high altitudes. They carry informations about the primary particle mass, the inelastic cross section and the fragmentation region of the interaction[1].

The observation of high energy muons in deep underground detectors is associated with studies in two different fields:

- Astrophysics, with studies of the spectrum and composition of primary cosmic rays in the energy region $10^{14} \leq E \leq 10^{17}$ eV.
- Particle physics, with studies of the features of the hadronic interactions at very high energy, in kinematical regions not accessible to accelerator experiments

(very forward region).

These lectures are an introduction to the phenomenology of particle astrophysics and include an overview of the most recent experimental results on multiple muons from underground experiments. A classic discussion on high energy muons fluxes and their measurement deep underground is in the review of Barret et al.[2]. Detailed calculations on this subject can be found in the T.K. Gaisser[3] textbook.

In the next section we briefly review the main characteristics of the high energy primary cosmic rays. In section 3 few concepts on ultra-high energy hadronic interactions are mentioned. Air showers are the subject of section 4. In particular, in this section, the characteristics of the muon component are discussed. Section 5 contains a review of a simplified treatment of muon propagation through matter. In sections 6 is shown the sensitivity of deep underground muons to primary composition and ultra-high energy hadronic interactions. Section 7 presents the main characteristics of different air shower codes widely used in modeling of underground muons. Section 8 contains a short description of the main characteristics of recent underground muon experiments and the presentation of experimental results on the study of high energy hadronic interactions and primary cosmic ray composition from multiple muon events measured in underground experiments.

2. Primary cosmic ray spectra

An introduction to high energy cosmic ray physics is presented in the dedicated lectures that can be found in these proceedings[4]. Here we briefly mention few general qualitative considerations about the characteristics of primary cosmic rays reaching the top of the atmosphere.

The cosmic rays incident on the atmosphere consist of protons and nuclei. The measured energy spectra, anisotropy, elemental and isotopic abundances (i.e. the relative fraction of protons with respect to heavy nuclei) of cosmic ray provide the basis from which a theoretical understanding of the origin of cosmic rays can be formulated. Up to now, the origin and acceleration processes are still unknown. The main sources are assumed to be supernovae, quasar and active galactic nuclei[3].

We have observations of the flux of cosmic ray particles in the range from 10^7 eV to 10^{20} eV. At 10^7 eV, the proton flux is known to be $\sim$1 proton/(m^2 s) while at 10^{20} eV is of the order of 1/(Km^2 century). This corresponds roughly to a drop of 15 order of magnitude. Both the total particle spectrum (all-particle spectrum) and the individual spectra of the component nuclei appear to approximately obey to a power law differential spectrum:

$$dN/dE \sim E^{-\gamma} \tag{1}$$

Up to approximately 1 PeV (1 PeV=10^{15} eV), γ is equal to $\sim$2.6. From 1 PeV to 10 EeV (1 EeV=10^{18} eV), the spectrum steepens to a γ of $\sim$ 3. Between 10 EeV and 40 to 50 EeV, it appears to flatten again with γ approaching $\sim$ 2.5. The first

break-point in the spectrum at around 1 PeV is conventionally called the "knee", while the second break at around 10 EeV is called the "ankle".

Different detection techniques are necessary to cover such a large energy range. At present, the cosmic ray energy spectra of individual elements are directly measured up to $\sim$ 100 TeV/nucleus (1 TeV=10^{12} eV). These experiments, which measure the absolute abundance and the elemental spectra of primary nuclei, use detectors carried on balloons and satellites[5]. Above 100 TeV the primary cosmic ray spectrum is of about one particle/(m^2 sr h). It decreases by a factor of about 50 for each decade of increase in energy. As a consequence, to achieve large enough exposure factors, in the UHE (Ultra-High Energy) region ($\geq 10^{14}$ eV/nucleus), the primary cosmic ray composition has to be inferred from the surface measurements of ground-based extensive air showers arrays[6] or from underground studies of the penetrating high energy muon component [9÷14]. Whereas the lower energy experiments at the top of the atmosphere directly detect the primary nuclei, the ground-based experiments perform indirect cosmic ray measurements, through the properties of secondary particles produced by the hadronic interactions of cosmic ray primaries with the atmosphere. The indirect nature of these experiments implies that modeling of the atmospheric cascades is essential to interprete the measurements and obtaining informations about primary composition and spectrum.

As mentioned above, a characteristic feature of the UHE region of cosmic ray spectrum is the steepening that occurs between 10^{14} and 10^{15} eV (the knee of the spectrum). Several explanations of this phenomenon have been formulated, many of which lead to substantial differences in the predicted shape of the spectrum near the knee. The interpretation of the knee may play a key role in understanding the origin of the cosmic rays in the whole energy range. Therefore, it is of great importance to reach definite conclusions about mass composition of primary cosmic rays around and above the "knee". Air shower and underground experiments, which can measure the whole region around the knee, are best suited for this purpose.

3. Ultra-High Energy hadronic interactions

A model for hadronic and nuclear interactions to be used in cosmic ray physics should provide the basic hadronic interaction term for the cosmic ray cascade, i.e. the cross section for hadron-hadron, hadron-nucleus and nucleus-nucleus collisions as a function of energy. The model should work from the pion production threshold up to the highest possible primary energies.

Results from collider and fixed target experiments at accelerators could provide important informations for a hadron production model to be used at cosmic ray energies. In table 1 the total center of mass energy ($\sqrt{s}$), corresponding to various proton laboratory energies (E_p) relevant for cosmic ray physics, are reported. Up to a proton energy $E_p \sim$ 1000 TeV, pp interactions are covered by existing pp ($p\bar{p}$)

collider experimental data. In the highest energy part of the region of interest, which corresponds to centre of mass energies $\sqrt{s} \approx 10$ TeV, i.e. supercollider (LHC) energies or greater, no direct collider measurements are available yet, and lower energy data have to be extrapolated. Nucleus-nucleus data from accelerator experiments need a much stronger extrapolation.

Table 1. Total center of mass energies corresponding to various proton energies.

E_p (TeV)	$\sqrt{s}$ (TeV)
1	0.043
10^1	0.137
10^2	0.433
10^3	1.37
10^4	~ 4
10^5	~ 10

Moreover, there are important differences between cosmic ray cascades and particle production at accelerators. At colliders, the central region in hadron-hadron collisions is usually best measured. In order to study the cosmic ray cascade, the main interest is in the forward fragmentation region of hadron-nucleus and nucleus-nucleus collisions, where multiple muons originate. At a typical underground depth, 30% of underground muons come from mesons at rapidity $y > 5$[7]. Therefore, extrapolations of the transverse momentum distribution in the fragmentation region from the central region measurements are also crucial to interpret multimuon data. Further elements of uncertainty in the extrapolation are the changes in the interaction features when nuclei are involved instead of single hadrons.

A review of the data on strong interactions from accelerator experiments most relevant for cosmic ray calculations can be found in Ref.[3] and in the proceedings of the lectures given by G. Battistoni[4].

4. Extensive Air Showers

An extensive air shower (EAS) is a cascade of particles generated by the interaction of a high energy cosmic ray proton or nucleus with air nuclei in the atmosphere: the number of particles at first multiplies, then reaches a maximum and attenuates as more and more particles fall below the threshold for further particle production. These particles move through the atmosphere, at nearly the speed of light, for many kilometers.

A cosmic ray induced shower has three components, electromagnetic, muonic and

hadronic. The shower consist of a core of high energy hadrons that continually feeds the electromagnetic part of the shower, primarily by photon from decay of neutral pions and η particles. Each high energy photon generates an electromagnetic subshower from alternate electron pair production and bremsstrahlung processes starting at its point of injection. Nucleons and other high energy hadrons contribute further to the hadronic cascade. Lower energy charged pions and kaons decay to feed the muonic component (the competition between decay and interaction depends on energy and depth in the atmosphere). Decays of π, k, μ are accompanied by neutrino production. Therefore also a neutral non interacting component participates to the shower development.

The point at which the incident cosmic ray interacts with an air nucleus is determined by its interaction length,which in turn is a function of the inelastic proton-air cross section (σ^{inel}_{p-air}) at the given energy. As we will show in the next sections, the muon component is directly coupled to the hadronic component of the EAS and, more directly than the electromagnetic component, reflects the properties of the initial hadron in the early development of the shower. This supports the interest in the underground muon experiments.

Details on the calculations of the fluxes of high energy hadrons, photons, muons and neutrinos in EAS can be found in Ref.[3].

4.1. The muon component of Extensive Air Showers

Muons in EAS are generated primarily from the decay of pions and kaons, through the interactions:

$$N + air \rightarrow \pi + X, K + X$$

and subsequent

$$\pi \rightarrow \mu, K \rightarrow \mu$$

decays, while only a very small fraction (few percent) of high energy muons are the result of direct (also known as prompt) production processes through charm and heavier flavour decays[a]

Therefore, the number of muons found in an extensive air shower depends on the relative likelihood that a pion (kaon) will decay rather than interact, and hence depends on the pion (kaon) energy and local air density.

At production heights of 5 Km, only pions of energy less than 30 GeV are more likely to decay than to interact; while at greater heights, where the air density is reduced, the decay probability also for higher energy pions increases.

Once produced, muons cross the atmosphere with a negligible probability of decaying and interacting (λ_{decay}=6200 E(TeV) Km, $\lambda_{int.} > 10^5$ g cm^{-1} for processes with

[a]Charmed particles have lifetimes so short that they almost always decay before interacting. This is why muons from decay of charm (and heavier flavours) are called prompt muons.

energy loss greater than 30%). It follows that the highest energy muons in EAS reflect processes occurring early in the shower development.

Furthermore, muons produced in EAS are linked to the chemical composition of the primary cosmic ray flux. In fact, the number of low energy (order of GeV) and high energy (order of TeV) muons in an EAS depends on the atomic number of the primary particle. The experimental muon properties, accordingly to their energy, can be summarized as follows:

- Low energy muons have reduced sensitivity to primary composition because they are generated in the latest stages of the hadronic shower development. In general, detectors for low energy muons from EAS use counters buried under ten or more meters of earth. This effectively absorbs the hadronic, electron and γ-ray components of the EAS. Detectors of this type can study the muon lateral distribution (i.e. the distance of the muons from the EAS longitudinal axis) and the muon multiplicity (i.e. the number of muons simultaneously detected in each event). The event rate is large, but the large spread of the muon shower (>100 m of radius) implies that an accurate measurement of the number of muons is difficult.

- High energy muons are very sensitive to primary composition. In general, the study of high energy muons from EAS is performed with deep underground detectors. The underground muon flux is relatively low, in particular for high energy events. Therefore, very large area detectors are needed.

The detection of the underground muons is the subject of these lectures. In the next sections we shall review the main properties of this component of EAS.

5. Energy loss of high energy muons through the rock

Interpretation of muon data for a given underground experiment depends on the detail of muon interaction processes occurring in the actual rock above the detector. Therefore, in order to study underground muons it is important to review muon propagation through matter. The brief review reported in this section is mainly derived from the T.K. Gaisser textbook[3]. A compilation of formulas and parameters for high energy muon energy loss in different materials can be found in the Lohmann et al. report[15].

Energy loss processes for high energy muons can be divided into two categories: continuous processes (ionization) and discrete processes (bremsstrahlung, electromagnetic interaction with nuclei and direct production of e^+e^- pairs). In the former processes the energy loss rate after penetrating a depth X of material, dE_μ/dX, is nearly constant for relativistic particles. For a numerical estimate of ionization loss of muons in rock $dE_\mu/dX = -\alpha$, with $\alpha \sim 2MeV/(g \cdot cm^{-2})$, can be used.

The discrete processes for muons are important only at high energy, and they are characterized by discrete burst along the muon trajectory. On average, the energy loss rate for this kind of processes is proportional to the muon energy E_μ. For muons, direct pair production is comparable to bremsstrahlung (or slightly more important than that). Inelastic electromagnetic interactions with nuclei (hadroproduction) are about a factor three less important.

In general, we can write the energy loss for muons as:

$$dE_\mu/dX = -\alpha - E_\mu/\xi, \tag{2}$$

where

$$\xi^{-1} = \xi^{-1}_{Bremss.} + \xi^{-1}_{Pair} + \xi^{-1}_{Had.},$$

and $\xi \approx 2.5 \times 10^5$ g/cm^2 in rock. Equating the two energy loss terms a critical energy $\epsilon = \alpha\xi$ can be defined. Above this energy discrete processes are more important than ionization process. In the rock, the muon critical energy is $\epsilon \sim 500$ GeV.

The general solution of Eq.(2) is:

$$< E_\mu(X) >= (E^0_\mu + \epsilon)\ e^{-X/\xi}\ -\ \epsilon, \tag{3}$$

which represents the mean energy of a beam of muons of initial energy E^0_μ after penetrating a depth X. The minimum energy required for a muon at surface to reach the depth X is the solution of Eq.(3) with residual energy $E_\mu(X) = 0$:

$$E^{thr.}_\mu = \epsilon\ (e^{X/\xi}\ -\ 1). \tag{4}$$

6. Deep underground muons

Underground muons are the high energy part of the muonic component of air showers. The rock overburden can be used as a filter to absorb not only the electromagnetic component, but also the strongly interacting components of the cosmic radiation and select muons having high average energy (the neutrino component of the EAS is also effectively selected). Fig. 1 shows the muon flux as a function of depth. For example, the average muon flux at Gran Sasso laboratory, in Italy (> 1100 m of rock), is $\sim 1\ \mu\ \mathrm{m}^{-2}\ \mathrm{h}^{-1}$, about 10^{-6} times the surface flux. The energy threshold for muons when they enter the ground in order to reach the underground detector is determined by the rock overburden. At Gran Sasso laboratory, using Eq.(4), the energy threshold is E_μ=1.3 TeV. This roughly corresponds to a primary cosmic ray energy threshold of about 10 TeV. Underground muons carry informations about the early development of the shower and preserve the feature of primary interactions, typically taking place at an average altitude of $\sim$ 17 Km above the observation level.

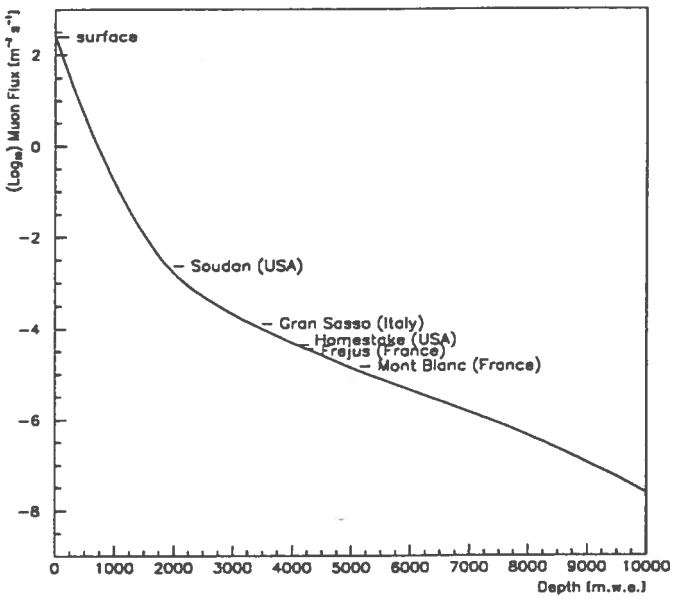

Figure 1: Atmospheric muon flux as a function of underground depth.

Occasionally, more than one muon of very great energy is produced in EAS, and when this happens, the muons follow nearly parallel paths close to the shower axis. The probability of such an occurrence increases rapidly with the primary energy. Such muons are detected as nearly parallel tracks in underground detectors. Of particular interest are those events having several multiple coincident ($\Delta t \leq$ ns) muons ("muon bundles")[17,16,18], typically separated by few meters[7].

As shown in the next two subsections, underground muon events illustrate some of the main issues of air shower physics in a particularly clear way. The most important one is the chemical composition of the primary cosmic rays above 100 TeV, which has not been measured in direct experiments (see section 2), due to the extremely low flux at high energy. Another fundamental issue is the study of hadronic interactions at energies well beyond those presently available in the laboratories.

6.1. Sensitivity of deep underground muons to UHE hadronic interactions

In the laboratory frame, muons propagate through the atmosphere in a narrow cone around the incident cosmic ray direction. At the earth surface, the average lateral distance of the muons from the shower axis <d> depends on energy ($E_{\pi,k}$) and interaction height (h) of the parent mesons as well as on their transverse momentum

(p_T) distribution:

$$< d > \approx h \frac{p_T}{E_{\pi,k}} \tag{5}$$

Deflection in the earth magnetic field also affects the muon lateral distribution (for muons with energy $\leq$500 GeV, i.e. for relatively shallow detectors). Underground, multiple Coulomb scattering in the rock (mostly important for extremely deep detectors) contributes to the lateral spread. At detector level the lateral spread may be several meters.

The lateral distribution of muons measured in large, powerful underground detectors is therefore sensitive to UHE hadronic interations. It can be used to test the hypotheses on the transverse momentum distribution of the parent pions and kaons. This measurement is important to validate the hadronic interaction models used in the simulation of multiple muons underground.

6.2. Sensitivity of deep underground muons to primary composition

The rates of muon bundles of different multiplicities measured in deep underground experiments are sensitive to the chemical composition and energy spectra of the primary cosmic rays, above an energy threshold determined by the rock overburden. This sensitivity arises from the fact that heavy nuclei tend to generate a larger yield of charged pions and kaons in the forward fragmentation region, as compared to that of light nuclei. The penetrating muons observed deep underground are produced by decays of these pions and kaons. At fixed cosmic ray energy, muons produced by light nuclei are more energetic than those produced by heavy nuclei[b], and hence they penetrate deeper into the earth. At high primary energy, however, also the muons from heavy nuclei are sufficiently energetic to penetrate to the depth of the detector. The energy where this crossover occurs depends upon the rock depth. Fig. 2 shows the muon yield of protons and iron primaries at two different depths, calculated from Ref.[8].

From this figure is evident that the multiplicity of underground muon events is determined by the primary cosmic ray mass and energy. In fact, muons reaching an underground detector, at a depth $\geq$ 1100 m of rock, typically have energies of several TeV at production in the atmosphere. This is an energy range in which low multiplicity events mostly come from protons and Helium nuclei with energies less than few hundred TeV. On the contrary, high multiplicity events reflect much higher primary energies ($\geq$ few 10^3 TeV), where heavy elements are more prolific than protons in producing TeV muons. Therefore, the primary energy region covered by muons observed deep underground includes the region of the knee of the spectrum (see section 2) and extends up to $\sim 10^{17}$ eV for the highest multiplicity events.

[b]This can be easily understood in the context of the superposition model for the treatment of the nuclear interactions. This model treats interactions of nuclei of total energy E and mass number A as A independent interactions of nucleons with energy E/A.

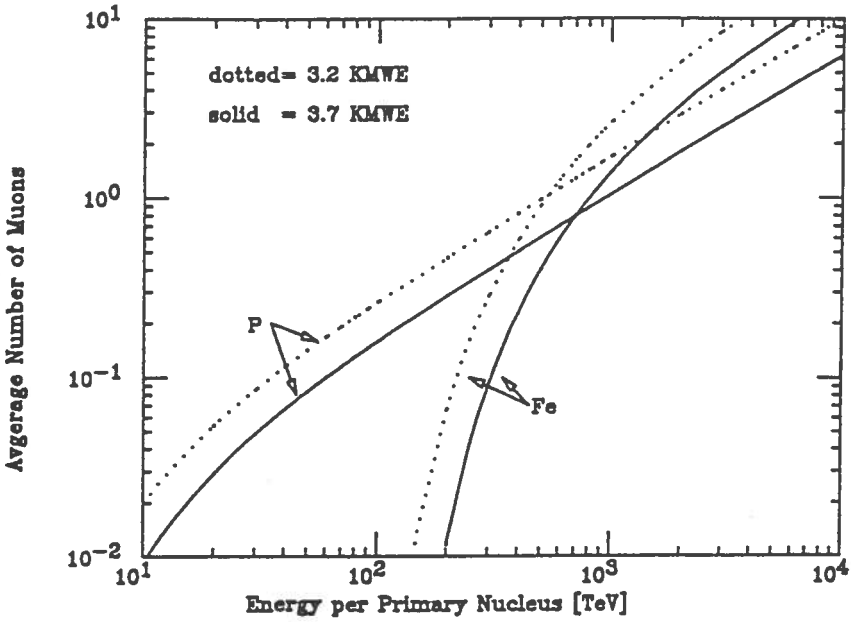

Figure 2: Muon yield at two different depths for p or Fe induced showers as a function of total primary energy per nucleus, calculated from Ref.[8]. Vertical incidence is assumed in the calculation.

With underground detectors, the energy and type of the primary cannot be determined on an event-by-event basis, but informations on mass composition can be obtained by means of Monte Carlo simulations, assuming different models of the primary spectrum and composition (trial models). Indications about most likely models are extracted by comparing measured muon multiplicity distributions with those calculated with the Monte Carlo simulations.

One should note that an important source of uncertainty in the data simulation comes from our limited knowledge of proton-air and nucleus-air inclusive meson production at very high energies (see section 3). The role of the hadronic interactions is of great importance, particularly when the detector is not large enough to contain the entire muon bundle. The transverse momentum distribution of the parent mesons used in the Monte Carlo code determines the expected fraction of muons above threshold that falls within the detector. If the average p_T is greater than the assumed one, it will result in a smaller muon density. This, in turn, will lead to a lower muon multiplicity in a given detector and so it might bias the resulting estimate of the composition.

6.3. Measurable quantities of underground muons

Underground muon experiments measure the muon multiplicity distribution and

the muon pair separation distribution. A finite size experiment has no knowledge of the position of the shower axis. Therefore the so-called decoherence function[19], frequency of all possible pairs of muons as a function of distance between them (in a bundle with N_μ muons there are $N_\mu(N_\mu - 1)/2$ independent pairs), which is strictly related to the lateral distribution, is measured instead of the lateral distance from the shower axis.

Results from simulation programs show that primary composition and hadronic interactions play a different role on muon measured parameters. Muon multiplicity distribution is largely determined by primary cosmic ray spectra and elemental composition, i.e. is weakly dependent on hadronic interaction mechanism. On the contrary, muon pair separation is primarily sensitive to energy and transverse momentum distribution of parent mesons (i.e. to the primary hadronic interaction) and to muon multiple scattering in the rock. This distribution is weakly dependent on primary composition.

7. Simulation of air showers

The indirect nature of the underground muon experiments means that modelling of atmospheric cascade is essential for the interpretation of any measurements.

Among various air shower simulation codes of hadronic interactions in atmospheric cascades, the HEMAS and SIBYLL programs are presently widely used for the simulation of underground muons. The HEMAS[8] program contains a hadron interaction event generator based on the parameterization of minimum bias event data, collected at the $Sp\bar{p}S$ collider by the UA5 experiment[20], generalized from single proton to nuclear targets. Multiplicity and pseudorapidity distributions from Monte Carlo calculations well reproduce collider data in the central region up to $\sqrt{s} \leq 900$ GeV. Projectile diffraction is included. In the original version of this code, the nuclear interaction is treated in the context of the pure superposition model[c] The treatment of the central region (pseudorapidity $\leq$5) in the energy region up to $\sqrt{s} \sim 1$ TeV is accurate, while the treatment of the forward region is based on extrapolations from much lower energy ($\sim$ 20 GeV) data of fixed target experiments. HEMAS is embedded in a shower simulation program which allows one to follow the shower development in the atmosphere with an energy cut on secondary particles down to 0.5 TeV. It also includes a three-dimensional muon propagation code in the rock.

The SIBYLL[21] event generator has been embedded in the same shower code already used for HEMAS. The SIBYLL model is more physically motivated than HEMAS, being based on the dual parton model [22], with the inclusion of hard processes such as mini-jet production [23].

Another air shower simulation program, CORSIKA[24], has been also originally based on the dual parton model. The present version allows the interface to other

[c]This approximation omits correlations which may be important in some context.

models (some of them however make use of similar concepts) adopted in the heavy ion physics, as VENUS[25]. It has also been interfaced to the EGS code[26] as a possibility to treat the electromagnetic part of the shower.

More recently the DPMJET interaction model[27] has been developed. It is also based on the two component (soft+hard scattering) dual parton model as SIBYLL, but with technical differences. A special care has been devoted to the the modelization of nuclear effects.

7.1. Parameterization of the features of muon events underground

The results of the simulation of air showers can be expressed in terms of parameterized formulas[1]. These parameterizations can be used in Monte Carlo simulations programs in place of the full event generator. This make possible to obtain predictions of multimuon data, at very little cost in CPU time. The parameterized formulas describe the main features of muon bundles underground as they would be observed in an infinite size detector, in particular their multiplicity distribution and lateral distribution as a function of the characteristics of the primary (mass, energy, and direction) and of rock depth.

For example, in HEMAS, a negative binomial distribution[8] fits the underground muon multiplicity distribution. This multiplicity distribution is close to a Poissonian (representation used in a previous model, described in Ref.[1]), but has an excess of events at high multiplicity (the "high multiplicity tail"). The average number of muons $< N_\mu >$ in the binomial multiplicity distribution can be expressed[28] as[d,e]

$$< N_\mu > \approx A \frac{0.0145\ TeV}{E_\mu^{thr.}\ cos\theta} \left(\frac{E_0}{A\ E_\mu^{thr.}}\right)^{0.757} \left(1 - \frac{A\ E_\mu^{thr.}}{E_0}\right)^{5.25}, \qquad (6)$$

where E_0 is the primary energy per nucleon in TeV, A is the primary mass, and $E_\mu^{thr.}$ is the energy threshold at the earth's surface (given by Eq.(4)).

The HEMAS muon lateral distribution (distance from shower axis), following what expected from the p_T distribution in hadronic collisions, is fitted by an inverse-power law form[8].

These parameterizations ignore the correlation between muon multiplicity and lateral distribution[f] Parameterizations can be useful to obtain a preliminary understanding of the data. The need of a better comprehension of the muon production processes and understanding the associated systematics leads preferably to the use of the full shower simulation codes. In this case the procedure to get usable Monte

[d]Note the dependence on the mass of the primary nucleus in this expression.
[e]The dependence on $E_0/E\mu^{thr.}$ comes from scaling hypothesis.
[f]Note that the correlation between altitude of production and muon multiplicity will introduce a correlation between multiplicity and separation of muons in an event.

Carlo predictions is complex and heavily CPU time consuming.

8. Results from underground muon experiments

The construction of large area, high resolution, underground proton-decay experiments has allowed the study of the rates of high energy multiple muons. The main characteristics of some of these detectors are reported in Table 2.

Table 2. Underground muon experiments.

Detector	Depth (m.w.e)	$E_\mu^{thr.}$ (TeV)	Size (m^2)	Granularity (cm)
BAKSAN[9]	850	0.22	16×16	70
FREJUS[10]	4850	3.7	6×12.3	0.5
HOMESTAKE[11]	4200	2.7	8×16	25
NUSEX[12]	5000	4.0	3.5×3.5	1
SOUDAN[13]	2090	0.8	130	2.5

These experiments achieved limited sensitivity to different trial compositions. The main reason is that these detectors are relatively small, and only a fraction of the muons in a high multiplicity event is typically detected. It is possible to improve the sensitivity to primary composition by using a larger area detector. In this way a larger fraction of muons in each event becames detectable, weakening the dependence on the assumptions about the transverse momentum distribution included in the simulation. Moreover, charm and heavier flavor particles, as discussed in section 4.1, could be responsible of muon production, through objects emitted at high transverse momenta. These processes not only increase the muon yields, but also generate more widely spreaded muon groups[1]. This illustrates the importance of exploring muon separation at distance as large as possible. Futhermore, by using a large area detector the sensitivity to primary composition also improves, increasing the muon rate and sampling of very high multiplicity events.

A much larger size detector, MACRO, mainly devoted to monopoles and cosmic ray detection, has been built at Gran Sasso laboratory, and is operational since 1989. A detailed description of the detector performances and physics results can be found in the lectures given by G. Giacomelli[29]. The MACRO detector, whose characteristics are described in Table 3, with its large detection area and excellent tracking capability, is well suited for high statistics studies of multiple muon events.

The role of the detector size in the measurements of underground muons is evident from Fig. 3, where the multimuon rates measured by the MACRO detector are

Table 3. MACRO experiment.

Detector	Depth (m.w.e)	$E_{\mu}^{thr.}$ (TeV)	Size (m^2)	Granularity (cm)
MACRO[14]	3700	1.4	12×77	3

shown[30].

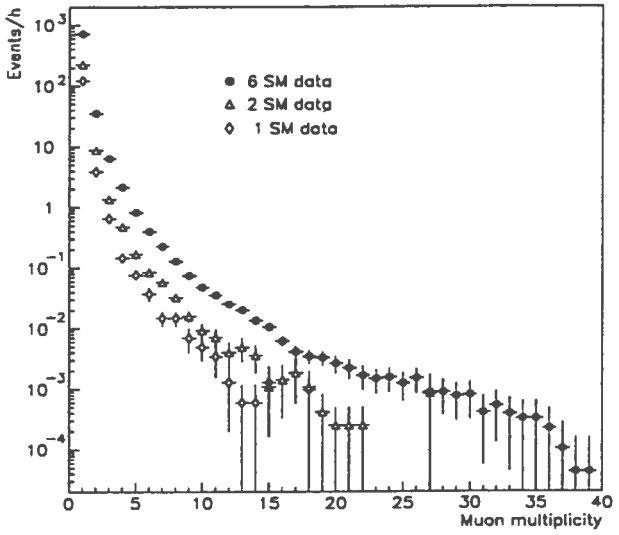

Figure 3: Multimuon rates for one (horizontal area 12 × 12 m^2), two (horizontal area 24 × 12 m^2) and six supermodules (horizontal area 76 × 12 m^2) MACRO data samples[30].

In this figure the distributions obtained for one supermodule (horizontal area 12 × 12 m^2), two supermodules (horizontal area 24 × 12 m^2) and six supermodules (horizontal area 76 × 12 m^2) event samples are shown. The increase in acceptance from one to six supermodules is reflected in an increase of muon rates and sampling of very high multiplicity and high separation events. The full-size MACRO detector (six supermodules), which is in operation since June 1991, collects $\sim 6.6\times10^6$ events per year of any multiplicity and, in particular, $\sim$ 400,000 events/yr with $N_{\mu} \geq 2$ and $\sim$ 1600 events/yr with $N_{\mu} \geq 10$. This allows one to reach a good statistical accuracy

on a very wide range of the primary energy spectrum.

8.1. The Muon decoherence function

The first important step in the analysis of multiple muon events underground, in view of composition studies, is the measurement of the decoherence function (see section 6.3).

The average hadronic p_T dependence on energy can be determined by measuring the decoherence function. Very large underground detectors (of the order of 1000 m^2) are clearly less biased by any lack of knowledge on p_T distribution. A comparison of data and Monte Carlo predictions allows an important validation of the model used for the composition analysis.

The decoherence distribution measured by a finite-size detector is biased by the dimensions of the detector. Pair separations that exceed the detector dimensions clearly cannot be measured, nor can separations less than the detector spatial resolution. A detector-independent decoherence function can be unfolded from the measured one, up to a maximum pair distance allowed by the apparatus, provided that the detector geometry and efficiency are properly considered in track reconstruction of the penetrating particles. The characteristics of the detector response can heavily affect the measured pair distance distribution. Therefore, only detector-independent data can be compared with the predictions of detector-independent Monte Carlo and/or other experimental data.

Experimental results have been produced by many experiments (see Table 2 and 3). The most significant are those from Frejus and MACRO Collaborations.

8.1.1. Frejus

The fine grained Frejus detector (0.5 cm resolution), located in the Frejus highway tunnel connecting Modane (France) and Bardonecchia (Italy), provided a clear separation of close packed muons. The Frejus detection area is (16×12.3) m^2, whereas the average distance between a muon pair at the Frejus depth is $\sim$ 5 m. In the Frejus analysis the observed lateral distribution is used to correct for detector size effects (as well as for other experimental biases), using a maximum likelihood method, and to obtain the true multiplicity distribution at the Frjeus site depth[17]. In this analysis the following assumption on the shape of the muon lateral distribution[31] is made:

$$\frac{dN}{dr} = \frac{r}{r_0^2}\, e^{-r/r_0} \tag{7}$$

where r is the distance between the muon and the unknown shower axis and r_0 is a characteristic distance to be fitted from the data. With this assumption the average distance between a muon and the shower axis is 2 r_0 and the average distance between two muons is (15/16 π) r_0. A correlation of r_0 with zenith angle is found, but not

with rock depth[9] A decrease in r_0 when the multiplicity varied from 2 to 4 is also shown by Frejus data. Above this multiplicity all fitted values of r_0 where found to be compatible with each other.

8.1.2. MACRO

The dimensions of the MACRO detector (76×12 m^2), are very large with respect to the average separation between muon pairs observed at Gran Sasso depth ($\sim$ 8 m). The large acceptance for downward muons and the excellent tracking capability ($\sim$1 cm average spatial resolution) of the MACRO detector make possible studies of the muon lateral distribution, which can be extended by one order of magnitude in separation over what was possible with previous underground experiments. MACRO has measured the decoherence function[7,32], defined as the rate of muon pair per unit area, per steradian, per pair separation determined on a plane orthogonal to the pair direction:

$$G(r) = \frac{1}{\Omega T} \int \frac{d^2 N_p(r,\theta,\phi)}{dr d\Omega} \frac{1}{A(\theta,\phi)} d\Omega \qquad (8)$$

where $d^2N_p(r,\theta,\phi)/drd\Omega$ is the density of pairs at distance r and incidence angle (θ,ϕ), A is the projected detector area in the (θ,ϕ) direction, Ω is the total solid angle defined by the limit of integration, and T is the exposure time.

Two different and independent methods have been used in this analysis to unfold the detector-independent decoherence function from the measured lateral separation. Fig. 4 shows the experimental decoherence curve for two supermodules, superimposed on the results of the Monte Carlo calculation using two different interaction models[7]. It can be seen that the lateral distribution of muon pairs shows sensitivity to the hadronic interaction models, allowing the rejection of some simplified cascade treatments[1], and also that the experimental data are reasonably described by the interaction model contained in the HEMAS[8] code.

Fig. 5 shows the experimental decoherence curve measured by the full MACRO detector[32], superimposed on the results of the Monte Carlo calculation using the HEMAS model and two rather "extreme" ("light": proton dominated, and "heavy": iron dominated) composition models[33]. As shown in this figure, the dependence of the muon decoherence function on the primary composition is small. The MACRO Collaboration has also investigated the dependence of the decoherence function from rock depth and zenith angle. The experimental and simulated data follow the same behaviour, and are close to each other. This gives some confidence about the capability of the HEMAS code to describe the right correlation between average transverse momentum, energy and production height of the parent mesons.

---

[9]Increasing the zenith angle the average separation is expected to increase, since higher production height are selected, while increasing the rock depth the average separation is expected to decrease, since higher muon energies in the atmosphere (reflecting higher primary energies) are selected.

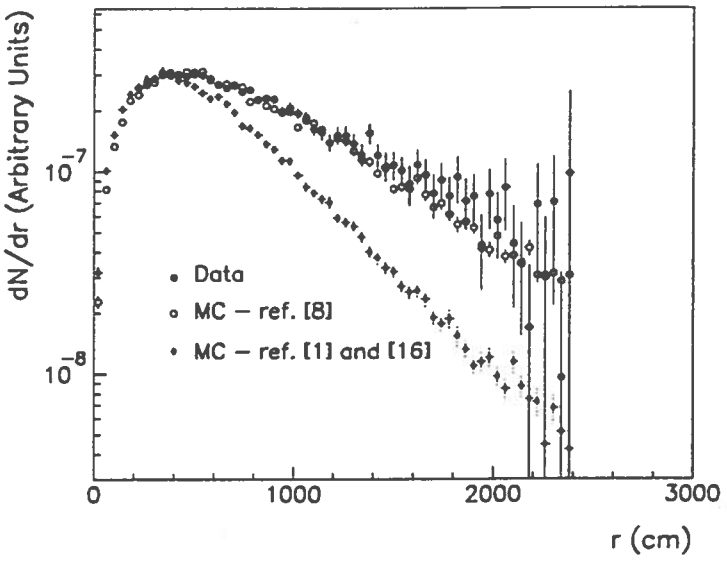

Figure 4: Comparison of the experimental (MACRO experiment, two supermodules data sample) decoherence distribution with simulations using two different hadronic interaction models[7].

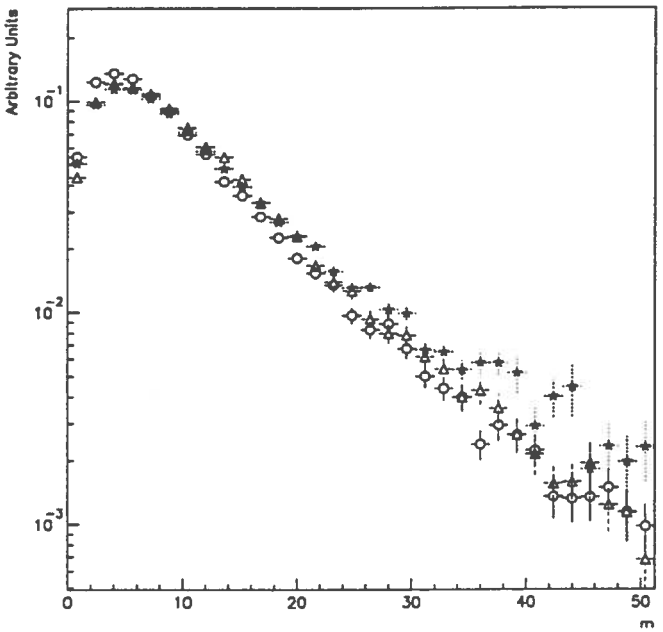

Figure 5: Comparison of the MACRO experimental (stars: six supermodules data sample) decoherence distribution with simulations using HEMAS and two composition models (open circles: "light" model, open triangles: "heavy" model)[32]

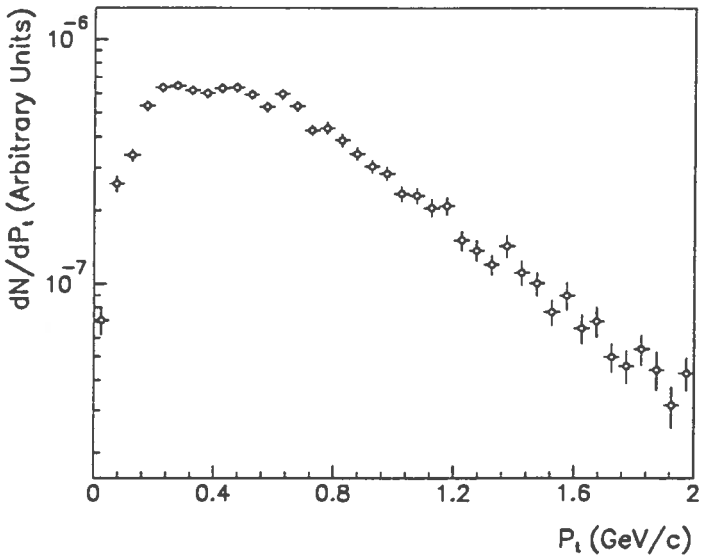

Figure 6: Distribution of the transverse momentum of the parent mesons giving at least two muons in MACRO (calculated using the HEMAS code)[7].

Fig. 6 shows the distribution of the transverse momentum of the parent mesons giving at least two muons underground, calculated using the HEMAS code. The average p_T value is $<p_T>$=550 MeV/c.

8.2. Primary Cosmic ray composition

The measurement of the primary cosmic ray composition is the main goal of any cosmic ray experiment. To access the higher energy regions of the primary spectrum, where the flux is low, large acceptance detectors are obviously required. Moreover, by performing combined measurements from underground experiments in coincidence with surface EAS arrays it is possible to obtain additional informations.

8.2.1. Homestake, NUSEX, Baksan

The Homestake detector, located in the Homestake Gold Mine, Lead, South Dakota, consists of a water Cherenkov counter and a liquid scintillation detector, with dimensions (8×16) m^2. The average separation between muon pairs at the Homestake site is $\sim$ 5 m. The Homestake Collaboration has analysed[34] their muon multiplicity rates, comparing the experimental data with Monte Carlo predictions, using parameterizations from the AIRSIM[h] code, for various composition models.

[h]Old code developed at Bartol and Utah by Gaisser, Elbert, Stanev et al.

This analysis indicates that a proton dominated composition is in better agreement with experimental data.

The NUSEX detector, located in the Mont Blanc tunnel, had a good granularity, but the dimensions of the detector were of the same order of magnitude of the average separation between muon pairs at the NUSEX site ($\sim$ 5 m). This means that the detector sampled only a small fraction of the muons in a multiple muon event and therefore the detector efficiency for high multiplicity events was very low. The NUSEX Collaboration has comparared the experimental muon rates with Monte Carlo simulations, using parameterizations from the HEMAS[8] code, for several different trial models of the primary spectrum and composition.

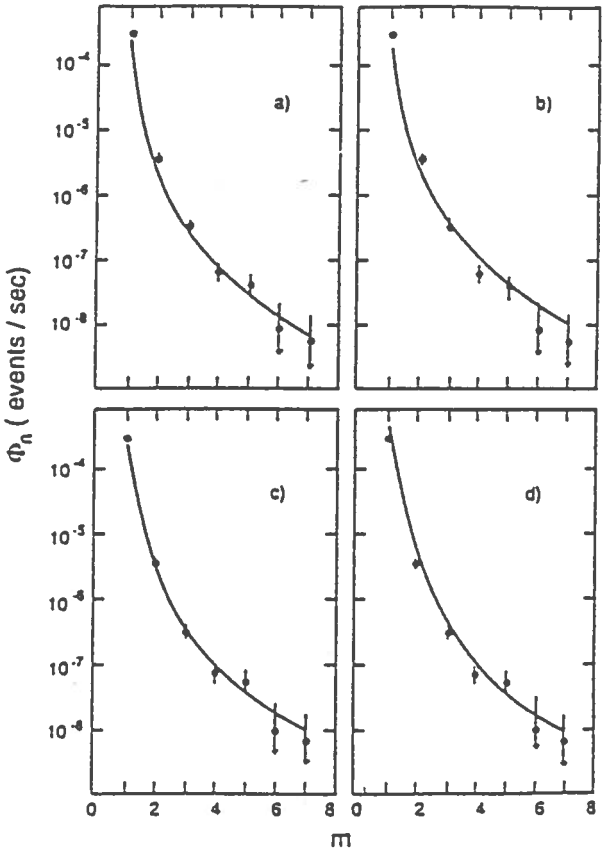

Figure 7: Comparison of the NUSEX experimental muon bundle rate with simulations using the HEMAS model and four different composition models: a) p-poor model; b) Maryland model; c) constant mass model; d) Linsley model[16].

The result of these analyses[16] is that the NUSEX data are in substantial agreement with simulation results, but none of the trial models is able to reproduce the whole set of experimental data. As it is shown in Fig. 7 it is difficult to reach a definite conclusion about composition on the basis of these multiple muon measurements. The dimensions of the Baksan scintillation telescope are of the same order of magnitude of the separation between muon pairs at Baksan depth ($\sim$ 13 m). The

Baksan Collaboration has reported[9] analyses based on the comparison of experimental muon rates with the results of a simulation, using a parameterization of the muon lateral distribution function. The result is that their experimental multiplicity distributions does not contradict a constant primary composition and constant spectral index (γ=2.7).

8.2.2. Surface-underground coincidence experiments

The possibility of detecting underground multiple muons in coincidence with the electromagnetic component of air showers in a surface EAS array experiment allows, in principle, a more constrained analysis. In fact, also the surface electromagnetic shower size N_e, for a given primary energy, preserve a composition dependence. This determines the overall improvement of the sensitivity to composition with the simultaneous measurement. At fixed primary energy, the heavy primaries (that interact at high altitude) generate showers which are attenuated earlier than those produced by protons, for the same reason they produce more muons. A simultaneous measurement of the underground number of muons N_μ and the surface shower size N_e will therefore correlate smaller N_e with higher N_μ for heavy primaries. The requirement of coincidence with surface array, however, unavoidably limits the angular acceptance of the surface-underground telescope and correspondingly the rate of the simultaneously detected events.

At Gran Sasso laboratory an interesting opportunity to perform a coincidence measurement[35] is given by the extensive air shower array experiment EAS-TOP at surface and the underground MACRO experiment. The high energy trigger of EAS-TOP allows the study of composition with an energy threshold around 100 TeV on primary cosmic rays. The coincident EAS-TOP and MACRO data are reasonably explained by the extrapolation of direct measurements of the primary cosmic rays (see section 2) performed at lower energies[36]. More consistent constraints will be established as soon as the statistical accuracy achieved in the coincidence experiment will be at the level of the systematic uncertainties.

Other coincidence experiments are the Soudan II nucleon decay detector and a surface air shower detector, the AMANDA and SPASE coincidence at the South Pole.

8.2.3. MACRO

MACRO multimuon events have been used in a first stage analysis[18,30] to study the primary cosmic ray composition by comparing the measured muon multiplicity distribution with those calculated using trial composition models. The main purpose of these studies was to investigate the detector sensitivity to primary composition. To this end the experimental data have been compared with two "extreme" hypotheses: a "light" (proton dominated) and a "heavy" (iron dominated) composition models[33].

The simulated events have been produced using the HEMAS hadronic interaction model, an accurate description of the rock depth distribution around the detector and a GEANT[37] based simulation program describing the geometry and detector response of the experimental apparatus. The comparison of the experimental data with Monte Carlo predictions showed good sensitivity of the MACRO detector to distinguish between primary cosmic ray compositions[18].

The six supermodules data sample contains many events of high multiplicity. This allows one to investigate correspondingly higher energy regions of the primary cosmic ray spectrum, above the "knee" region, where the knowledge of primary composition is still rather poor. MACRO multimuon events are produced by primaries in the energy range of ~ 50 to $\sim 10^5$ TeV. Fig. 8 shows the calculated range of primary energy that corresponds to the detection of 90% of events for each detected multiplicity in six supermodules [30]. This figure shows that the primary energies explored by the detection of multiple muons increases with muon multiplicity. In particular events with detected multiplicity $N_\mu \geq 10$ originate from primaries in an energy region entirely above the "knee".

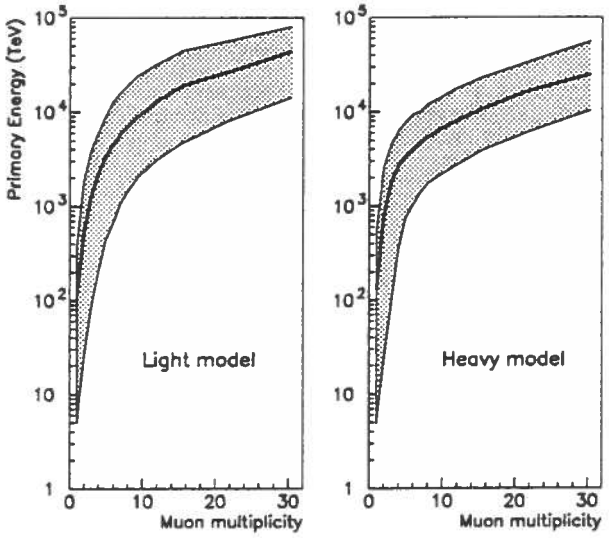

Figure 8: Calculated range of primary energy for the detection of 90% of MACRO events vs. multiplicity. The bold line gives the mean primary energy as a function of the detected multiplicity[30].

The expected rates obtained with the Monte Carlo simulation at each multiplicity are shown in Fig. 9, compared with the experimental data for six supermodules.

Experimental data lie in between the two models at lower multiplicities and favor the light model at higher multiplicity, showing a clear preference towards this composition for $N_\mu \geq 15$. A similar preference toward light composition has been

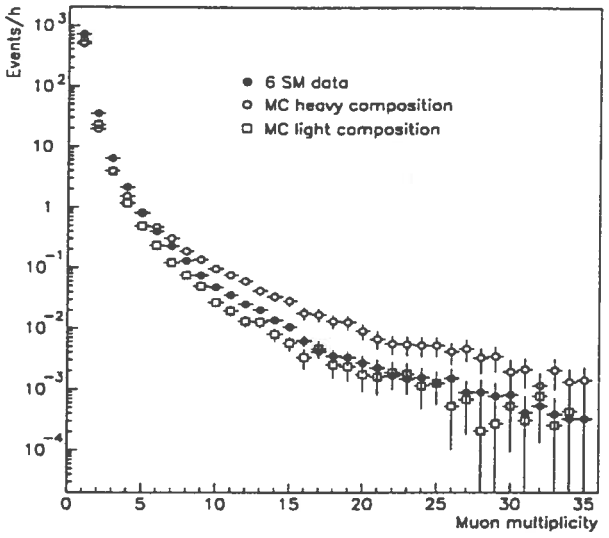

Figure 9: Comparison of the MACRO (six supermodules) experimental muon bundle rate with simulations using the HEMAS model and two composition models ("light" and "heavy")[30].

found comparing the calculated rates of muons at Frejus site with the experimental observations[38].

In a recent analysis the MACRO Collaboration has used a new approach for measuring the primary composition, making use of a multi-parametric fit of the multimuon data[41]. The parameters of the fit define the cosmic rays chemical composition. Therefore, this is the most direct approach to determine the primary composition from multimuon events. However it required a good statical precision, even at very high multiplicity, only very recently reached.

A wide energy interval of about one decade below the knee is available where direct measurements and underground muon measurements of the primary cosmic ray composition overlap. Therefore, in the fitting procedure data from direct experiments are used as starting points to constrain the composition below the knee. The minimized function is:

$$\chi^2 = \lambda_M \chi^2_M + \lambda_D \chi^2_D \tag{9}$$

where χ^2_M applies to MACRO multimuon data,

$$\chi^2_M = \sum_{N_\mu} \frac{[R^{meas}(N_\mu) - R(N_\mu \mid parameters)]^2}{\sigma^2[R^{meas}(N_\mu)] + \sigma^2[R(N_\mu \mid parameters)]} \tag{10}$$

χ^2_D applies to direct flux measurements,

$$\chi^2_D = \sum_A \sum_{i=1}^{N_A} \frac{[\Phi_A^{meas}(E_i) - \Phi_A(E_i \mid parameters)]^2}{\sigma^2[\Phi_A^{meas}(E_i)]} \tag{11}$$

and λ_M and λ_D are fixed weight parameters. In the fitting procedure λ_M is set equal 1 and λ_D has been varied between 0 and 1.

The predicted multimuon rates are calculated as:

$$R(N_\mu) = \Omega S \sum_A \int dE \Phi_A(E) P_A(E, N_\mu) \tag{12}$$

where Ω is the accepted solid angle, S is the sampling area, $\Phi_A(E)$ is the differential primary cosmic ray flux of the nucleus of mass A; and $P_A(E, N_\mu)$ is the probability for a nucleus of mass A and energy E to produce an event with N_μ reconstructed muons. The energy spectrum of each elemental group can be expressed by simple power laws, whose spectral indices change at a mass dependent knee energy:

$$\Phi_A(E) = K_1(A) E^{-\gamma_1(A)} \qquad for\ E < E_{cut}(A) \qquad and$$

$$\Phi_A(E) = K_2(A) E^{-\gamma_2(A)} \qquad for\ E > E_{cut}(A)$$

with $K_2 = K_1 E_{cut}^{\gamma_2 - \gamma_1}$. Assuming that primaries can be described using five mass groups (H, He, CNO, Mg, Fe), this corresponds to a maximum number of 20 parameters to be fitted. The number of parameters can be reduced according to specific physical hypotheses.

The $P_A(E, N_\mu)$ probabilities are calculated using the HEMAS code[8] with the "semi-superposition" model[39] for the treatment of the nuclear interactions. For comparison, also the SIBYLL interaction model[21] has been used. The multiplicity distributions calculated with HEMAS and SIBYLL exhibit similar behaviours, with single muon rates slightly higher in SIBYLL and multiple muon rates slightly higher in HEMAS. The inclusive muon flux calculated with SIBYLL is about 6 % higher than that calculated with HEMAS.

Fig. 10 shows the all-particle spectrum[i] arising from the multi-parametric fit for $\lambda_D = 0.01$. The χ^2/DoF is 14/24.

It can be easily recognized that the fitted spectrum is higher and flatter than the one obtained from direct measurements alone ($\lambda_M = 0$, $\lambda_D = 1$), exceeding it by an amount ranging from 15 % at E = 10 TeV to 50 % at E = 100 TeV, in agreement with the MACRO previous analysis[30]. A remarkable feature of the reconstructed all-particle spectrum, which derives from the fitting procedure, is the consistency with EAS measurements[40] around and above the knee. It has to be emphasized that these measurements, that are shown in Fig. 10 for comparison, are not used in the

[i] Because of its steepness, it is customary to display the differential spectrum multiplied by the energy raised to a power. This has the advantage of allowing an expanded vertical scale.

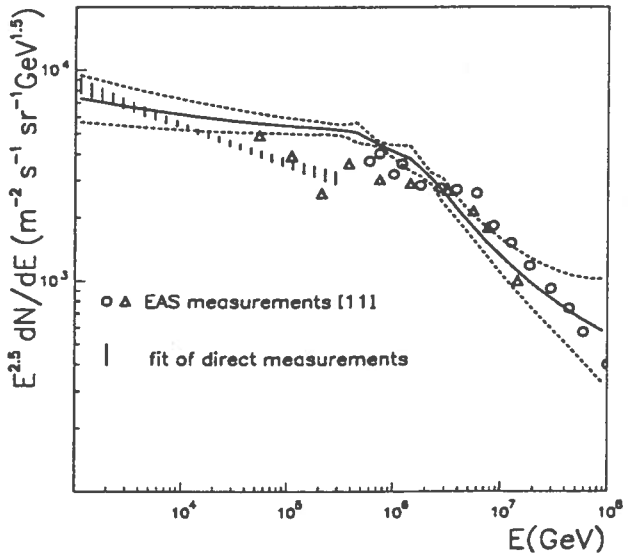

Figure 10: All particle spectrum of primary cosmic rays, derived from the multi-parametric fit procedure (MACRO experiment)[41].

minimized function. Indeed, the all-particle spectrum clearly shows the sensitivity of MACRO data to the knee. To prove this a different fit under the assumption of a single power law for each group (corresponding to 10 free parameters) has been performed. A χ^2/DoF of 60/30 was obtained, to be compared with 14/24 in the case of the two spectral index hypothesis.

Fig. 11 shows the <A> dependence on the primary energy for the same parameters used in Fig. 10. The relative abundances of the each elemental group at different primary primary energies have been reported in Ref.[41]. Both <A> and the relative abundances of each elemental group show a weak dependence on the primary energy below 10^6 GeV. Even within larger uncertainties MACRO data support a possible increase of the average mass number at higher energies.

9. Conclusions

The general features of underground muon physics are reasonably understood and well reproduced in Monte Carlo simulations. The present underground muon experiments have shown their capability to give a confident answer to the composition problem. MACRO detector size provide better statistics than the earlier measurements, allowing an unbiased study of muon lateral distribution. This is an essential step to give confidence to the study of primary cosmic ray composition. MACRO has demonstrated its ability to discriminate between different cosmic ray primary compositions. Moreover more definite conclusions have been obtained using the multi-parametric fit

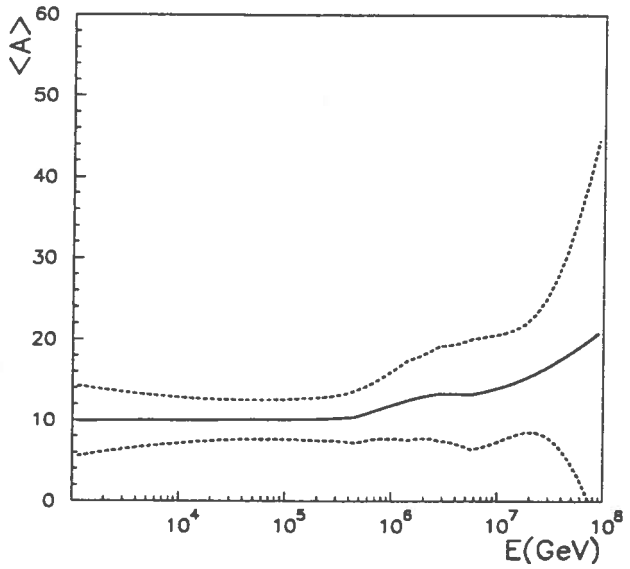

Figure 11: Average mass number of primary cosmic rays, derived from the multi-parametric fit procedure (MACRO experiment)[41].

method. This new method is a successful tool to "measure" the primary cosmic ray composition from multimuon events.

10. Acknowledgments

We are grateful to our colleagues of the MACRO Collaboration for many interesting discussions on underground muon physics. We thank F. Cavanna for reading this review and offering very helpful suggestions.

11. References

1. T.K. Gaisser and T. Stanev, *Nucl. Instr. & Meth.* **A235** (1985) 183.
2. P.H. Barret et al., *Revs. Mod. Phys.* **24** (1952) 133.
3. T.K. Gaisser, *Cosmic Rays and Particle Physics*, Cambridge University Press, Cambridge, England (1990).
4. G. Battistoni and A. Grillo, *Introduction to High Energy Cosmic Ray Physics*, these proceedings.
5. Asakimori et al., *Proc. of 23rd ICRC*, Calgary, **2** (1993) 21; Asakimori et al., *Proc. of 23rd ICRC*, Calgary, **2** (1993) 25; Zatsepin et al., *Proc. of 23rd ICRC*, Calgary, **2** (1993) 13; Ichimura et al., *Proc. of 23rd ICRC*, Calgary, **2** (1993) 5; Ichimura et al., *Proc. of 23rd ICRC*, Calgary, **2** (1993) 9; Ivanenko et al., *Proc. of 23rd ICRC*, Calgary, **2** (1993) 17;
6. Kakimoto et al., *Proc. of 23rd ICRC*, Calgary, **2** (1993) 103; Astrashkevich et al., *Proc. of 23rd ICRC*, Calgary, **2** (1993) 116.
7. S. Ahlen et al.,*Phys. Rev.* **D46** (1992) 4836.
8. C. Forti et al., *Phys. Rev* **D42** (1990) 3668.
9. A.E. Chudakov et al., *Proc. of 22nd ICRC*, Dublin, **2** (1991) 5.
10. Ch. Berger et al., *Nucl. Instr. & Meth.* **A262** (1987) 463.
11. M.L. Cherry et al., *Phys. Rev.* **D27** (1983) 1444.
12. G. Battistoni et al., *Nucl. Instr. & Meth.* **A245** (1986) 277; (Proc. Suppl.) **14B** (1990) 193.
13. Longley et al., Proc. of 23rd ICRC, Calgary, **2** (1993) 120.
14. S. Ahlen et al., *Nucl. Instr. & Meth.* **A234** (1993) 337.
15. W. Lohmann , R. Kopp and R. Voss, *CERN report* **85-05** (1985).
16. G. Bologna et al., *Nuovo Cimento* **8C** (1985) 76. M. Aglietta et al., *Nucl. Phys.*
17. Ch. Berger et al., *Phys. Rev.* **D40** (1989) 2163.
18. S. Ahlen et al.,*Phys. Rev.* **D46** (1992) 895.
19. P. Sokolsky, *Introduction to Ultrahigh Energy Cosmic Ray Physics*, Addison-Wesley Publishing Company, Inc. (1989).
20. G.J. Alner et al., *Phys. Lett.* **167B** (1986) 476.
21. R.S. Fletcher et al., *Phys. Rev* **D50** (1994) 5710.
22. See for instance A. Capella et al., *Phys. Rev. Lett.* **58** (1987) 2015, and references therein.
23. T.K. Gaisser and T. Stanev, *Phys. Lett.* **B219** (1989) 375.
24. J.N. Capdevielle et al., *the Karlsruhe extensive air shower simulation code CORSIKA*, KFK Report 4998 (1992).
25. K. Werner, Phys. Rep. **232** (1993) 87.
26. W.R. Nelson et al., SLAC Report 265 (1984).
27. I. Kawrakov et al., *Phys. Rev* **D47** (1993) 3849.

28. J.W. Elbert, *Proc. DUMAND Summer Workshop* (ed. A. Roberts) **vol.2** (1978) 101.
29. G. Giacomelli, *The MACRO experiment at Gran Sasso*, these proceedings.
30. S. Ahlen et al., in *Proc. of 23rd ICRC*, Calgary, 2 (1993) 97.
31. J.W. Elbert, T.K. Gaisser, and T. Stanev, *Phys. Rev* **D27** (1983) 1448.
32. S. Ahlen et al., in *Proc. of 23rd ICRC*, Calgary, 2 (1993) 93.
33. G. Auriemma et al., in *Proc. of 21st ICRC*, Adelaide, **9** (1990) 362.
34. D.B. Kieda Ph.D thesis (1989).
35. R. Bellotti et al., *Phys. Rev.* **D42** (1990) 1396.
36. M. Aglietta et al., *Phys. Lett.* **B337** (1994) 376.
37. R. Brun et al., *GEANT3 manual*, CERN DD/EE/84-1.
38. G. Auriemma et al., in *Proc. of 22nd ICRC*, Dublin, OG6.2.1 (1991).
39. J. Engel et al., *Phys. Rev.* **D46** (1992) 5013.
40. Compilation of EAS data by Hillas, A.M., Annu. Rev. Astron. Astrophys. **22** (1984) 425.
41. S. Ahlen et al., in *Proc. of 24th ICRC*, Rome, 2 (1995) 689.